Author Manuscript

Author Manuscript

Author Manuscript

Author Manuscript

HHS Public Access

Author manuscript

Cancer Res. Author manuscript; available in PMC 2017 May 31.

Published in final edited form as:

Cancer Res. 2009 February 15; 69(4): 1587–1595. doi:10.1158/0008-5472.CAN-08-2915.

Effective Immunotherapy against Murine Gliomas Using Type 1 Polarizing Dendritic Cells—Significant Roles of CXCL10

Mitsugu Fujita[1,7], **Xinmei Zhu**[1,7], **Ryo Ueda**[1,7], **Kotaro Sasaki**[3,4], **Gary Kohanbash**[1,6,7], **Edward R. Kastenhuber**[1,7], **Heather A. McDonald**[1,7], **Gregory A. Gibson**[6], **Simon C. Watkins**[6], **Ravikumar Muthuswamy**[4], **Pawel Kalinski**[2,4,6], and **Hideho Okada**[1,2,7]

[1]Department of Neurological Surgery, University of Pittsburgh Cancer Institute, Pittsburgh, Pennsylvania

[2]Department of Surgery, University of Pittsburgh Cancer Institute, Pittsburgh, Pennsylvania

[3]Department of Dermatology, University of Pittsburgh Cancer Institute, Pittsburgh, Pennsylvania

[4]Department of Immunology, University of Pittsburgh Cancer Institute, Pittsburgh, Pennsylvania

[5]Department of Cell Biology and Physiology, University of Pittsburgh School of Medicine, Pittsburgh, Pennsylvania

[6]Department of Infectious Diseases and Microbiology, University of Pittsburgh Graduate School of Public Health; Pittsburgh, Pennsylvania

[7]Department of Brain Tumor Program, University of Pittsburgh Cancer Institute, Pittsburgh, Pennsylvania

Abstract

In an attempt to develop effective vaccines against central nervous system (CNS) tumors, we evaluated the ability of vaccines with standard dendritic cells (DC) versus type 1 polarizing DCs (DC1) to induce glioma-specific type 1 CTLs with CNS tumor-relevant homing properties and the mechanism of their action. C57BL/6 mouse-derived bone marrow cells were cultured with mouse granulocyte/macrophage colony-stimulating factor (GM-CSF) for 6 days, and $CD11c^+$ cells were subsequently cultured with GM-CSF, rmIFN-γ, rmIFN-α, rmIL-4, and polyinosinic-polycytidylic acid stabilized by lysine and carboxymethylcellulose for 24 hours to generate DC1s. In analogy to their human counterparts, mouse DC1s exhibited surface marker profiles of mature DCs and produced high levels of IL-12 and CXCL10. Importantly for their application as cancer vaccines, such DC1s stably retained their type 1 phenotype even when exposed to type 2-promoting or regulatory T cell (Treg)-promoting environments. Consistently, mouse DC1s induced antigen-specific type 1 CTLs more efficiently than nonpolarized DCs *in vitro*. DC1s given s.c. migrated into draining lymph nodes, induced antigen-specific CTLs, and suppressed Treg accumulation. In addition, s.c. immunization with DC1s loaded with glioma-associated antigen (GAA)-derived CTL epitope peptides prolonged the survival of CNS GL261 glioma-bearing mice, which was

Requests for reprints: Hideho Okada, G12a Research Pavilion at Hillman Cancer Center, 5117 Center Avenue, Pittsburgh, PA 15213. Phone: 412-623-1111; Fax: 412-623-4747; E-mail: okadah@upmc.edu.

Note: Supplementary data for this article are available at Cancer Research Online (http://cancerres.aacrjournals.org/).

Disclosure of Potential Conflicts of Interest: No potential conflicts of interest were disclosed.

Author Manuscript Author Manuscript Author Manuscript Author Manuscript

associated with efficient CNS glioma homing of antigen-specific CTLs. Intratumoral injections of GAA peptide-loaded DC1s further enhanced the anti-CNS glioma effects of DC1-based s.c. immunization. Interestingly, the antitumor functions were abrogated with *CXCL10*$^{-/-}$ mouse-derived DC1s. Collectively, these findings show the anti-CNS glioma effects of DC1-based therapy and a novel role of CXCL10 in the immunologic and therapeutic activity of DC-based cancer vaccines.

Introduction

Malignant gliomas represent the most common primary central nervous system (CNS) tumors and exhibit a dismal prognosis despite recent advances made in surgical, radiological, and chemotherapeutic approaches (1). Development of novel, multi-modal therapeutic approaches is, thus, critical to improve the outcome of these deadly tumors (2). Among these approaches, immunotherapy can be promising for glioma treatment if we are able to induce potent immune responses directed against glioma-associated antigens (GAA; refs. 3–5). Indeed, several immunologic strategies have been evaluated in early-phase clinical trials; however, modest clinical outcomes of glioma immunotherapy trials call for further improvement of strategies (6).

The rejection of CNS gliomas by GAA-targeted vaccines is initiated by sufficient expansion of GAA-specific effector T cells. Vaccine-induced GAA-specific T cells are then required to home to CNS glioma sites in sufficient numbers, retain their functionality, and exert their antitumor activities. In this regard, we have previously shown that intratumoral (i.t.) injections of dendritic cells (DC) transduced with *IFN*-α cDNA enhance anti-CNS tumor immunity not only by promoting cross-presentation of tumor-associated antigens in draining lymph nodes (DLN; refs. 7–9) but also by enhancing CNS tumor homing of antigen-specific type 1 CTLs through the induction of CXCL10, a type 1 chemokine (10, 11). These observations point to the significance of promoting type 1 adaptive immunity for anti-CNS tumor immunotherapy.

In an attempt to develop effective vaccines against CNS tumors, we evaluated the ability of DC-based vaccines with standard DCs versus type 1 polarizing DCs (DC1) to induce glioma-specific type 1 CTLs with CNS tumor-relevant homing properties and the mechanism of their action *in vivo*.

Whereas human DC1s show an excellent ability to induce Th1 and CTL responses (12–14), the mechanism of their action remains unclear. In particular, although human DC1s have been recently shown to produce diminished levels of regulatory T cell (Treg)– attracting chemokines but enhanced levels of chemokines attracting Th1 cells, CTLs, and natural killer (NK) cells (15, 16), the role of chemokine production in the overall effectiveness of DC1-based vaccines has not been evaluated.

In the current study, mouse DC1s exhibit superior therapeutic activity against GL261 gliomas *in vivo*. Moreover, we show that the anti-CNS glioma effects by DC1-based therapy depend on CXCL10 production by DC1s. This novel mouse DC1 system allows us to address how DC1-based therapy can be applied for glioma patients and points to the

Author Manuscript Author Manuscript Author Manuscript Author Manuscript

significance of CXCL10 production as a critical release criterion for patients' autologous DC1s in vaccine trials.

Materials and Methods

Reagents

RPMI 1640, fetal bovine serum (FBS), L-glutamine, sodium pyruvate, β-mercaptoethanol, nonessential amino acids, antibiotics, and carboxyfluorescein diacetate succinimidyl ester (CFSE) were obtained from Invitrogen Life Technologies. Recombinant mouse granulocyte/macrophage colony-stimulating factor (rmGM-CSF), rmIFN-α, rmIL-10, rmIL-12, and rmCXCL10 were obtained from R&D Systems. Recombinant human IL-2 (rhIL-2), rmIFN-γ, and rmTGF-β1 were obtained from PeproTech. Lipopolysaccaride (LPS) was obtained from Sigma-Aldrich. Polyinosinic-polycytidylic acid stabilized by lysine and carboxymethylcellulose (poly-ICLC) was kindly provided by Oncovir. The following peptides were synthesized by the automated solid-phase peptide synthesizer at University of Pittsburgh Peptide Synthesis Facility: H-2K^b-binding EphA2$_{682-689}$ (VVSKYKPM), H-2D^b-binding Garc1$_{77-85}$ (AALLNKLYA), H-2D^b-binding human/mouse gp100 (h/mgp100)$_{25-33}$ (KVPRNQDWL), and H-2K^b-binding ovalbumin (OVA)$_{257-264}$ (SIINFEKL).

Cell culture

CD40L$^+$ J558 mouse myeloma cell line was used in the current study (13). *TAP2*$^{-/-}$ RMA-S mouse thymoma cell line was kindly provided by Dr. Walter J. Storkus (University of Pittsburgh; ref. 17). GL261 mouse glioma cell line was kindly provided by Dr. Robert Prins (University of California-Los Angeles); GL261 cells are of C57BL/6 mice (H-2^b)-background and express mgp100, EphA2, and Garc-1 as GAAs (18-20). GL261 culture supernatants were filtered and concentrated 10-fold by using an Amicon Ultra Filter (Millipore). GL261-conditioned medium was then prepared by mixing the concentrated supernatants and fresh medium at a ratio of 1:9. All cells were maintained in mouse complete medium (RPMI 1640 supplemented with 10% heat-inactivated FBS, 100 units/mL penicillin, 100 mg/mL streptomycin, and 10 μmol/L L-glutamine) in a humidified incubator in 5% CO_2 at 37°C.

Animals

Wild-type C57BL/6 mice (H-2^b) were obtained from Taconic Farms. Pmel-I, *IL-12p35*$^{-/-}$, *CXCL10*$^{-/-}$, and *green fluorescent protein*-transgenic (*GFP*-Tg) mice, which are all of C57BL/6-background, were obtained from The Jackson Laboratory. Pmel-I mice are transgenic for an hgp100$_{25-33}$-specific TCR that cross-reacts to an mgp100$_{25-33}$/H-2K^d complex (21).

Antibodies and gp100-specific tetramer

The following antibodies were obtained from BD Biosciences: anti-CCR5 (C34-3448), anti-CD11c (HL3), anti-CD40 (HM40-3), anti-CD8 (53-6.7), anti-CD80 (16-10A1), CD86 (GL1), H-2K^b (AF6-88.5), anti-I-A^b (AF6-120.1), anti-IFN-γ (XMG1.2, anti-IL- 4 (11B11), and isotype-matched controls. Anti-CCR7 (4B12) and anti-Gr-1 (RB6-8C5) antibodies were obtained from BioLegend. Anti-CXCR3 (220803) antibody was obtained

Author Manuscript Author Manuscript Author Manuscript Author Manuscript

from R&D Systems. Anti-CD11b (M1-70), anti-FoxP3 (FJK-16s), and anti-granzyme B (16G6) antibodies were obtained from eBioScience. H-2D^b/hgp100$_{25-33}$ tetramer was obtained from National Institute of Allergy and Infectious Disease Tetramer Facility at Emory University Vaccine Center.

Flow cytometry

The procedure used in the current study has been described previously (10). Briefly, single-cell suspensions were surface-stained with fluorescent dye-conjugated antibodies. For intracellular staining, cells were surface-stained, washed, fixed, permeabilized with Cytofix/Cytoperm buffer (BD Biosciences), and intracellularly stained. All stained cells were compared with those stained with isotype-matched control antibodies. Samples were examined by Coulter EPICS cytometer (Beckman Coulter); data were analyzed by the WinMDI software.8

Cytokine and chemokine release assay

The ELISA kits obtained are as follows: mIL-12p70 from eBioscience; mCXCL10, mCCL5, and mCCL22 from R&D Systems; and mIFN-γ from BD Biosciences. Culture supernatants were evaluated by specific ELISA kits.

In vitro DC preparation

The protocol used in the current study was established on the basis of our previous studies with additional procedures for DC1 generation (11, 22). Bone marrow cells (BMC) were cultured in complete medium supplemented with 10 ng/mL mGM-CSF. The medium and supplements were replaced every 3 d. On day 6, immature DCs (iDC) were purified by positive selection with CD11c magnetic beads (Miltenyi Biotec). Mature, standard DCs (sDC) were then generated by further 24-h cultivation of CD11c$^+$ DCs with 250 ng/mL LPS and 10 ng/mL mGM-CSF. DC1s were generated from iDCs by further 24-h cultivation with 5 μg/mL poly-ICLC and 10 ng/mL each of rmIFN-γ, rmIFN-α, and rmIL-4.

In some experiments, to stimulate IL-12p70 production by DCs, CD40L$^+$ J558 cells were added in culture at a J588/DC ratio of 1:5. In some experiments, DCs were loaded with 5 μg/mL hgp100$_{25-33}$, Garc1$_{77-85}$, or a combination of Garc1$_{77-85}$ and EphA2$_{682-689}$ peptides, incubated for 4 h at 37°C, and washed twice with PBS. In s.c. immunization experiments, on days 0 and 10, recipient mice received s.c. injections of 1×10^6 DCs loaded with GAA-derived peptides mentioned above with 100 μL PBS.

In vivo DC migration assay

DCs were generated from C57BL/6-background *GFP*-Tg mice; in some experiments, DC1s were generated from either wild-type or *CXCL10*$^{-/-}$ mice and labeled with 0.1 μmol/L CFSE. On day 0, recipient mice received s.c. injection of 3×10^6 DCs in 0.1 mL PBS without peptide loading. At 48 h, GFP$^+$ or CFSE$^+$ cells in DLNs were evaluated by flow cytometry.

[8] http://facs.scripps.edu/software.html

Author Manuscript Author Manuscript Author Manuscript Author Manuscript

In vitro CTL preparation

The procedure used in the current study has been described previously (23). Briefly, $CD8^+$ T cells were enriched from Pmel-I mouse-derived spleen cells (SPC) by positive selection with CD8 magnetic beads (Miltenyi Biotec) and stimulated with DCs loaded with 5 μg/mL $hgp100_{25\text{-}33}$ peptide in the presence of 100 units/mL rhIL-2. $CD8^+$ T cells were cultured at 6 to 9 d for *in vitro* cytolytic assay and 8 to 12 d for i.v. injection.

In vitro cytolytic assay

The procedure used in the current study has been described previously (11). Briefly, target RMA-S cells were pulsed with 5 μg/mL of either $mgp100_{25\text{-}33}$ or $OVA_{257\text{-}264}$ peptide and labeled with 100 μCi $Na_2^{51}CrO_4$ (Amersham). The labeled cells (100 μL) were then incubated with effector cells (100 μL) in a U-bottomed 96-well microtiter plate (Corning). After a 4-h incubation at 37°C, 50 μL supernatants were harvested from each well and transferred to wells of a LumaPlate-96 (Packard, Inc.). The amount of ^{51}Cr in each well was measured in a Microplate Scintillation Counter (Packard, Inc.). The percentage of antigen-specific cytolysis was calculated as follows: 100 × (experimental release − spontaneous release) / (maximum release − spontaneous release).

In vivo CTL proliferation assay

On day – 1, wild-type mice received i.v. injection of 5×10^6 Pmel-I mouse-derived, naive $CD8^+$ T cells labeled with 1 μmol/L CFSE. On day 0, mice received s.c. immunization with DCs loaded with 5 μg/mL $hgp100_{25\text{-}33}$ peptide. On day 6, proliferation of $CFSE^+$ cells in DLNs was evaluated by flow cytometry.

In vivo cytolytic assay

The procedure used in the current study has been described previously (24). Briefly, on day 0, wild-type mice received s.c. immunization of DCs loaded with 5 μg/mL $Garc1_{77\text{-}85}$ peptide. On day 6, SPCs were obtained from naive C57BL/6 mice and divided into two groups: (*a*) a $CFSE^{hi}$ group, consisting of SPCs pulsed with 5 μg/mL $Garc1_{77\text{-}85}$ peptide, incubated for 1 h at 37°C, and labeled with 1 μmol/L CFSE, and (*b*) a $CFSE^{lo}$ group, consisting of SPCs labeled with 0.1 μmol/L CFSE without peptide loading. Mice then received i.v. injection of 1×10^7 cells from each group. At 4 h, SPCs were evaluated by flow cytometry for the proportion of $CFSE^{lo}$ and $CFSE^{hi}$ cells.

Intracranial injection of GL261 glioma cells, DCs, and rmCXCL10

The procedure used in the current study has been described previously (10,23, 24). Briefly, using a Hamilton syringe (Hamilton Company), 1×10^5 GL261 cells in 2 μL PBS, 1 to 3×10^6 DCs in 2 μL PBS, or 1 μg rmCXCL10 in 1 μL PBS were stereotactically injected through an entry site at the bregma, 3 mm to the right of sagittal suture, and 4 mm below the surface of the skull of anesthetized mice by using a stereotactic frame (Kopf). In some experiments, symptom-free survival was monitored as the primary end point; in other experiments, treated mice were sacrificed on indicated days to evaluate immunologic end points, such as brain infiltrating lymphocytes (BIL).

Author Manuscript Author Manuscript Author Manuscript Author Manuscript

BIL isolation

The procedure used in the current study has been described previously (25). Briefly, mice were sacrificed by CO_2 asphyxia and immediately perfused with PBS through the left cardiac ventricle. Brain tissues were mechanically minced, resuspended in 70% Percoll (Sigma-Aldrich), overlaid with 37% and 30% Percoll, and centrifuged for 20 min at 500 × *g*. Enriched BIL populations were recovered at the 70% to 37% Percoll interface.

Two-photon excitation microscopy

The Olympus FV1000MPE multi-photon laser scanning microscope (Olympus Corp.) was used to image GFP in sections of brain tissues and cervical lymph nodes (CLN). The Olympus Fluoview software controlled data acquisition. The mode-locked Chameleon Ultra Ti:Sapphire laser (Coherent, Inc.) produced illumination for two-photon excitation at 820 nm. The Olympus 60-fold objective with numerical aperture of 0.70 was used with a 2-fold digital zoom to optically section tissue at a 2-μm step size. Fluorescence emission was collected with an external photomultiplier tube using a 520/40 nm bandpass filter. Scan resolution was set to 1,024 × 1,024 pixels at 4,096 gray scales.

Statistical analysis

The statistical significance of differences between groups was determined by one-way ANOVA with Holm's post-hoc test. Survival data were analyzed by log-rank test. We considered differences significant when $P < 0.05$. All data were analyzed by the R environment.[9]

Results

Requirements for cytokines and TLR ligands in the generation of mouse DC1s

We first determined the requirements for a combination of cytokines and TLR ligands to polarize mouse DC1s effectively. As DC maturation markers, we evaluated DC expression of the following molecules: MHC class II (I-A^b), costimulatory molecule CD80, and chemokine receptor CCR7, which primarily mediates DC migration toward DLNs (26). We also measured DC production of IL-12p70, which is a key cytokine for type 1 adaptive immunity (26). As shown in Supplementary Fig. S1, the expression of maturation markers and production of IL-12p70 depended greatly on TLR3 ligand poly-ICLC and IFN-γ; at lesser degrees on IFN-α and IL-4. Therefore, we used poly-ICLC, IFN-γ, IFN-α, and IL-4 for the generation mouse DC1s in the current study, as detailed in Materials and Methods.

Mouse DC1s stably retain their type 1 polarizing phenotype when exposed to type 2–promoting or Treg-promoting environments

We characterized mouse DC1s for their production of cytokines and chemokines, as well as their surface phenotype *in vitro*. As shown in Fig. 1A, compared with iDCs, both sDCs and DC1s exhibited higher levels of MHC class I (H-2K^b) and class II (I-A^b), costimulatory molecules CD80/86, and the chemokine receptor CCR7, which is consistent with mature DC

[9] http://www.r-project.org/

Author Manuscript Author Manuscript Author Manuscript Author Manuscript

phenotype. As shown in Fig. 1B, DC1s produced significantly higher levels of type 1 cytokine IL-12p70 and type 1 chemokines CXCL10 and CCL5 than sDCs or iDCs upon stimulation with CD40L. By contrast, DC1s suppressed the production of CCL22, a chemokine that primarily attracts Tregs (16, 27). As shown in Fig. 1C, when these DCs were subsequently exposed to type 2–promoting or Treg-promoting factors (IL-10, TGF-β, or GL261 glioma-conditioned media), only DC1s were able to maintain their production of IL-12p70 and CXCL10. Collectively, these data show that mouse DC1s stably retain their type 1 polarizing phenotype even when they are subsequently exposed to type 2–promoting or Treg-promoting environments.

Mouse DC1s efficiently induce antigen-specific type 1 CTLs *in vitro*

We then evaluated the ability of mouse DC1s to induce type 1 effector CTLs through their antigen presentation *in vitro* (Fig. 2). DC1s, control sDCs, or iDCs were loaded with hgp100$_{25\text{-}33}$ peptide and cocultured with Pmel-I mouse-derived, gp100$_{25\text{-}33}$-specific CD8$^+$ T cells. DC1s induced superior levels of intracellular IFN-γ, granzyme B, and CXCR3 in responder CD8$^+$ T cells when compared with sDCs or iDCs, whereas the expression levels of IL-4 and CCR5 were comparable in DC1-stimulated versus sDC-stimulated CD8$^+$ T cells (Fig. 2A). Furthermore, DC1-stimulated T cells produced significantly higher levels of IFN-γ in culture supernatants (Fig. 2B) and exhibited a superior antigen-specific CTL activity against both antigen-pulsed RMA-S cells and syngeneic GL261 cells (Fig. 2C) when compared with sDC-stimulated or iDC-stimulated cells.

Mouse DC1s efficiently migrate into DLNs, induce antigen-specific CTLs, and suppress the accumulation of Tregs *in vivo*

We subsequently evaluated the ability of GAA peptide-loaded DC1s to induce antigen-specific CTLs *in vivo* (Fig. 3). As shown in Fig. 3A, at 48 h after s.c. immunization with DCs derived from *GFP*-Tg mice, GFP $^+$ DC1s were found in DLNs at higher numbers than sDCs or iDCs, which is consistent with the high-level expression of CCR7 on DC1s (Fig. 1A). As shown in Fig. 3B, CFSE-labeled, Pmel-I– derived CD8$^+$ T cells exhibited a higher degree of proliferation after s.c. immunization with hgp100$_{25\text{-}33}$-loaded DC1s than immunization with sDCs or iDCs. *In vivo* CTL assays with Garc1$_{77\text{-}85}$ peptide showed that DC1-based s.c. immunization induced higher levels of Garc1$_{77\text{-}85}$-specific CTL responses (Fig. 3C) than sDC-based or iDC-based immunization. DC1-based immunization also led to a reduction of FoxP3$^+$CD4$^+$ Tregs that accumulated in DLNs (Fig. 3D), suggesting that the DC1s that migrated into DLNs may modulate the overall immunologic milieu, perhaps as a result of their type 1 chemokine production profiles (Fig. 1). Collectively, these data show that mouse DC1s efficiently migrate into DLNs, induce antigen-specific CTLs, and may suppress the accumulation of Tregs in DLNs.

Peripheral immunization with DC1s prolongs survival of CNS glioma-bearing mice associated with the efficient CNS glioma homing of antigen-specific CTLs

We next evaluated whether DC1-based peripheral s.c. immunization would promote effective therapeutic immunity against CNS GL261 gliomas (Fig. 4). CNS GL261-bearing mice received s.c. immunization with 1×10^6 DC1s, sDCs, or iDCs loaded with GL261 glioma-derived CTL epitope peptides, Garc-1$_{77\text{-}85}$ (H-2D^b), and EphA2$_{682\text{-}689}$ (H-2K^b), on

Author Manuscript Author Manuscript Author Manuscript Author Manuscript

days 0 and 10 after the intracranial inoculation of GL261 glioma cells. As shown in Fig. 4A, immunization with GAA peptide-loaded DC1s prolonged the survival of CNS glioma-bearing mice significantly longer than that with sDCs, iDCs, or mock PBS treatment. When the immune cell infiltration in CNS glioma sites was examined using naive Pmel-I–derived $CD8^+$ T cells adoptively transferred and their relevant $hgp100_{25\text{-}33}$-loaded DCs (Fig. 4*B*–D), DC1-based s.c. immunization resulted in a significant increase of antigen-reactive $CD8^+$ T cells but a decrease of $FoxP3^+CD4^+$ Tregs and $Gr\text{-}1^+CD11b^+$ myeloid suppressor cells in CNS glioma sites when compared with sDC-based or iDC-based immunization. Collectively, these data show that peripheral s.c. immunization with DC1s prolongs the survival of CNS glioma-bearing mice, which was associated with the efficient CNS glioma homing of antigen-specific CTLs.

Intratumoral injection of DC1s enhances anti-CNS glioma effects of s.c. immunization with DC1s

We subsequently addressed whether i.t. injections of DC1s would promote or enhance the therapeutic efficacy against CNS GL261 gliomas. To this end, we first examined the persistence of DC1s after i.t. injections. As shown in Fig. 5A, i.t. injected GFP^+ DC1s seemed to persist better than sDCs in both the CNS glioma sites and CLNs, which are regional DLNs of the brain. We then addressed whether i.t. injections of DC1s would prolong the survival of CNS glioma-bearing mice. As shown in Fig. 5B, both s.c. and i.t. DC1 injections prolonged the survival of CNS glioma-bearing mice better than mock PBS injections. Remarkably, the combination of both s.c. and i.t. DC1 injections resulted in the highest long-term survival rate with 5 of 10 mice surviving at day 100 after tumor inoculation. When we examined the infiltration of antigen-reactive $CD8^+$ T cells in CNS glioma sites (Fig. 5C), s.c. injections of DC1s recruited significantly higher numbers of antigen-reactive $CD8^+$ T cells when compared with i.t. injections alone. Addition of i.t. DC1 injections in the s.c. DC1 regimen led to a further improvement of T cell homing to the CNS glioma sites. Collectively, these data show that i.t. injections of DC1s enhance anti-CNS glioma effects of DC1-based s.c. immunization.

DC1-derived CXCL10 plays a significant role in both induction of antigen-specific CTLs and their CNS glioma homing

Based on our previous observations (10, 11), we hypothesized that CXCL10 produced by i.t. injected DC1 would play a major role in CNS glioma homing of antigen-specific CTLs. We generated *CXCL10*$^{-/-}$ mouse-derived DC1s that exhibited similar surface expression levels of MHC class II ($I\text{-}A^b$), CD80, and CCR7 compared with wild-type DC1s (Fig. 6A, *top*). *CXCL10*$^{-/-}$ DC1s were able to migrate to DLNs after s.c. injections as efficiently as wild-type DC1s (Fig. 6A, *bottom*).

To our surprise, as shown in Fig. 6B, s.c. immunization with GAA peptide-loaded *CXCL10*$^{-/-}$ DC1s induced decreased levels of antigen-reactive $CD8^+$ T cells, as shown by enumeration in DLNs (*top*), proliferation (*center*), and antigen-specific cytolytic ability (*bottom*) of *in vivo* induced CTLs compared with wild-type DC1s, indicating that CXCL10 plays a role in the induction of antigen-specific CTLs.

Author Manuscript Author Manuscript Author Manuscript Author Manuscript

We subsequently examined the significance of CXCL10 produced by DC1s in the s.c. immunization model. As shown in Fig. 6C, lack of DC1-derived CXCL10 partially abrogated the therapeutic effects of DC1-based s.c. immunization (*top*; $P = 0.0936$ compared with the no DC control group), which was associated with the decreased CNS glioma homing of antigen-reactive $CD8^+$ T cells (*bottom*).

We then examined the significance of CXCL10 produced by DC1s in the i.t. injection model. As shown in Fig. 6D, DC1-derived CXCL10 was at least partially responsible in the therapeutic effects and CNS glioma homing of antigen-reactive $CD8^+$ T cells, as shown by injections of *CXCL10*$^{-/-}$ DC1s. In a group of mice receiving *CXCL10*$^{-/-}$ DC1s, coinjections of rmCXCL10 recovered the therapeutic efficacy and CNS glioma homing of antigen-specific $CD8^+$ cells.

Collectively, these data show a major role of DC1-derived CXCL10 both in the systemic induction of antigen-specific CTLs and their CNS glioma homing.

Discussion

In the current study, we focused on the development of DC1-based therapeutic strategies for gliomas. The results shown here support our hypothesis that immunization with GAA peptide-loaded DC1s promotes desirable type 1 adaptive immune responses against CNS gliomas, with the effects being significantly dependent on the DC production of CXCL10. In particular, a combination approach of s.c. immunization with and i.t. injection of DC1s showed remarkable anti-CNS glioma effects (Fig. 5), indicating the possibility to use DC1s to jointly target the afferent and efferent phases of immune responses.

Several protocols to generate DC1s from mouse BMCs have been proposed previously (28, 29). Compared with other mouse DC1s, our DC1s generated in the current study exhibited the following unique and novel biological properties: (*a*) high-level production of not only IL-12 but also type 1 chemokines, such as CXCL10 (Fig. 1B) and (*b*) commitment to produce IL-12 and CXCL10 even when they are exposed to IL-10, TGF-β, or glioma-conditioned medium (Fig. 1C). These data indicate that mouse DC1s share the hallmark characteristics of human αDC1 in terms of their ability to produce type 1 cytokines and chemokines at high levels (12, 15).

Of great interest is the observation that CXCL10 is required in the CNS glioma homing, as well as the induction of effector CTLs (Fig. 6A and B), because its receptor CXCR3 is expressed on activated T cells at high levels (30). In this regard, Dufour and colleagues have shown the role of CXCL10 in both the induction and homing of effector T cells using *CXCL10*$^{-/-}$ mice (31). They hypothesized two possible mechanisms by which CXCL10 influences the induction of effector T cells. One possibility is that CXCL10 may influence DC migration to DLNs, thereby affecting CTL induction. However, our observation does not support this possibility because both wild-type and *CXCL10*$^{-/-}$ DC1s migrate to DLNs at a comparable efficiency (Fig. 6A). The other possibility is that CXCL10 may costimulate T-cell activation in an autocrine loop because activated effector T cells also release CXCL10 (32). In our current models with *CXCL10*$^{-/-}$ DC1s, T cells in the recipient wild-type mice

Author Manuscript Author Manuscript Author Manuscript Author Manuscript

should be able to produce CXCL10. Nevertheless, s.c. immunization with *CXCL10*$^{-/-}$ DC1s failed to induce antigen-specific CTLs, pointing the significance of DC1-derived CXCL10 for induction of adaptive immune responses. Gustasfsson and colleagues have reported recently that αDC1s attract NK cells *in vitro* in a manner dependent on CXCR3, which is a receptor for CXCL10, leading to IFN-γ production from NK cells (15). Therefore, it may be due to the lack of NK-cell recruitment to the DLNs and their IFN-γ production that s.c. immunization with *CXCL10*$^{-/-}$ DC1s failed in CTL induction (Fig. 6B). We have recently reported that effector CTLs, but not memory T cells, kill antigen-loaded DCs in DLNs in an antigen-specific manner, thereby diminishing the effect of DC-based immunization (33). However, this is not likely to be the case in the current study because the *CXCL10*$^{-/-}$ DCs might not be able to attract effector CXCR3^{+} CTLs efficiently. Precise mechanisms by which DC1-derived CXCL10 promotes the induction of effector CTLs DC1s need to be elucidated.

In addition to CXCL10, other DC1-derived factors may play a pivotal role in inducing type 1 immune response. We and others have described DC-derived IL-12 as a critical factor in the induction of type 1 immunity (26, 34). To corroborate this point in our current mouse DC1 model, we generated DC1s from *IL-12p35*$^{-/-}$ mice (Supplementary Fig. S2). Absence of functional IL-12p70 production almost completely abrogated abilities of DC1s to induce type 1 CD8^{+} T-cell response *in vitro* and therapeutic efficacy, as well as T-cell trafficking to the CNS tumors *in vivo*. With regard to other DC1-derived chemokines, it was recently reported that human αDC1s overproduce CXCL9-11 and CCL5, which altogether contribute to the induction of type 1 immune response (15). It is, therefore, possible that these chemokines contribute to the observed beneficial effects in our glioma-bearing mice as well. Further studies are clearly warranted to elucidate the roles of these chemokines. Human αDC1s produce reduced levels of CCL22, thereby diminishing attraction of Tregs (16). These may explain our observation in the current study that immunizations with mouse DC1s resulted in reduced accumulation of Treg cells in DLNs (Fig. 3D).

DCs need to be licensed by CD40-CD40L engagement to induce a burst of IL-12, as shown by our previous study (13). However, in the current study, we did not use CD40L stimulation of DCs to evaluate their ability to induce CTL responses *in vitro*. This is because, in our preliminary studies, *in vitro* stimulation of DC1s with CD40L^{+} J558 cells resulted in the death of both DC1s and T cells even when relatively few CD40L^{+} J558 cells were used. We reason that supraphysiologic levels of CD40-CD40L engagement in mouse DC/T-cell interaction *in vitro* may induce excessive production of IL-12 followed by IFN-γ, leading to the overproduction of nitric oxide, to which mouse immune cells are highly susceptible (35-37). However, our *in vivo* DC1 administrations consistently resulted in superior levels of CTL induction compared with other DC types, suggesting that the excessive CD40-CD40L interaction may not be a concern *in vivo*.

Our data in Fig. 5 suggest that i.t.-given DC1s may induce antigen-specific CTL responses in draining CLNs. Based on our data with s.c. injected *CXCL10*$^{-/-}$ DC1s, we presume that i.t. injected DC1s also depend on endogenous CXCL10 for the induction of antigen-specific CTLs. Accordingly, i.t. injection of *CXCL10*$^{-/-}$ DC1s did not induce significant therapeutic responses (Fig. 6C). On the other hand, complementary administration of rmCXCL10 along

Author Manuscript Author Manuscript Author Manuscript Author Manuscript

with i.t. *CXCL10*$^{-/-}$ DC1 delivery recovered the therapeutic effects of i.v. type 1 CTL transfer (Fig. 6D). We think this was because the adoptive transfer of *in vitro* activated type 1 CTLs bypassed the necessity of endogenous CTL induction, which might have been diminished in mice receiving i.t. *CXCL10*$^{-/-}$ DC1s. Therefore, the observed recovery of CTL infiltration to the glioma site is likely due to the local chemoattractive effects of rmCXCL10.

In our experiments with i.t. DC1 injections, we loaded DC1s *ex vivo* with synthetic GAA-derived peptides. Based on our previous study (8) and the current data (Fig. 5A), i.t. injected DC1s seem to migrate into CLNs, regional DLNs of the brain, wherein they present antigen to reactive T cells. One may raise a question whether DC1s needed to be loaded with exogenous peptides to elicit therapeutic responses in spite of abundant availability of tumor antigens *in situ*. Immature DCs are highly phagocytic. During their maturation process, however, DCs lose the ability to engulf antigens while they gain the ability to migrate into DLNs and present antigens to naive T cells efficiently (26). Our DC1s exhibited mature DC phenotype (Fig. 1A) and, thus, might not be highly phagocytic. Therefore, in the current study, we elected to load DC1s *ex vivo* with synthetic GAA-derived peptides. However, it remains to be determined whether DC1s are able to phagocytose and present tumor-derived antigens efficiently.

In summary, the current study shows that mouse DC1s can induce superior therapeutic activity against CNS GL261 gliomas *in vivo* and that CXCL10 production is significant to the *in vivo* effectiveness of cancer vaccines.

Supplementary Material

Refer to Web version on PubMed Central for supplementary material.

Acknowledgments

Grant support: Grants 1R01NS055140-01, 1P01CA100327, and 1P01NS40923 (H. Okada); 1R01CA095128 (P. Kalinski).

References

1. Stupp R, Mason WP, van den Bent MJ, et al. Radiotherapy plus concomitant and adjuvant temozolomide for glioblastoma. N Engl J Med. 2005; 352:987–96. [PubMed: 15758009]
2. Selznick LA, Shamji MF, Fecci P, Gromeier M, Friedman AH, Sampson J. Molecular strategies for the treatment of malignant glioma-genes, viruses, and vaccines. Neurosurg Rev. 2008; 31:141–55. [PubMed: 18259789]
3. Eguchi J, Hatano M, Nishimura F, et al. Identification of interleukin-13 receptor α2 peptide analogues capable of inducing improved antiglioma CTL responses. Cancer Res. 2006; 66:5883–91. [PubMed: 16740728]
4. Okano F, Storkus WJ, Chambers WH, Pollack IF, Okada H. Identification of a novel HLA-A*0201-restricted, cytotoxic T lymphocyte epitope in a human glioma-associated antigen, interleukin 13 receptor α 2 chain. Clin Cancer Res. 2002; 8:2851–5. [PubMed: 12231526]
5. Hatano M, Eguchi J, Tatsumi T, et al. EphA2 as a glioma-associated antigen: a novel target for glioma vaccines. Neoplasia. 2005; 7:717–22. [PubMed: 16207473]
6. Carpentier AF, Meng Y. Recent advances in immunotherapy for human glioma. Curr Opin Oncol. 2006; 18:631–6. [PubMed: 16988586]

Author Manuscript Author Manuscript Author Manuscript Author Manuscript

7. Tsugawa T, Kuwashima N, Sato H, et al. Sequential delivery of interferon-α gene and DCs to intracranial gliomas promotes an effective antitumor response. Gene Ther. 2004; 11:1551–8. [PubMed: 15343358]
8. Okada H, Tsugawa T, Sato H, et al. Delivery of interferon-α transfected dendritic cells into central nervous system tumors enhances the antitumor efficacy of peripheral peptide-based vaccines. Cancer Res. 2004; 64:5830–8. [PubMed: 15313927]
9. Kuwashima N, Nishimura F, Eguchi J, et al. Delivery of dendritic cells engineered to secrete IFN-α into central nervous system tumors enhances the efficacy of peripheral tumor cell vaccines: dependence on apopto-tic pathways. J Immunol. 2005; 175:2730–40. [PubMed: 16081851]
10. Nishimura F, Dusak JE, Eguchi J, et al. Adoptive transfer of type 1 CTL mediates effective anti-central nervous system tumor response: critical roles of IFN-inducible protein-10. Cancer Res. 2006; 66:4478–87. [PubMed: 16618775]
11. Fujita M, Zhu X, Sasaki K, et al. Inhibition of STAT3 promotes the efficacy of adoptive transfer therapy using type-1 CTLs by modulation of the immunological microenvironment in a murine intracranial glioma. J Immunol. 2008; 180:2089–98. [PubMed: 18250414]
12. Vieira PL, de Jong EC, Wierenga EA, Kapsenberg ML, Kalinski P. Development of Th1-inducing capacity in myeloid dendritic cells requires environmental instruction. J Immunol. 2000; 164:4507–12. [PubMed: 10779751]
13. Mailliard RB, Wankowicz-Kalinska A, Cai Q, et al. α-type-1 polarized dendritic cells: a novel immunization tool with optimized CTL-inducing activity. Cancer Res. 2004; 64:5934–7. [PubMed: 15342370]
14. Wesa A, Kalinski P, Kirkwood JM, Tatsumi T, Storkus WJ. Polarized type-1 dendritic cells (DC1) producing high levels of IL-12 family members rescue patient T_H1-type antimelanoma $CD4^+$ T cell responses *in vitro*. J Immunother. 2007; 30:75–82. [PubMed: 17198085]
15. Gustafsson K, Ingelsten M, Bergqvist L, Nystrom J, Andersson B, Karlsson-Parra A. Recruitment and activation of natural killer cells *in vitro* by a human dendritic cell vaccine. Cancer Res. 2008; 68:5965–71. [PubMed: 18632652]
16. Muthuswamy R, Urban J, Lee JJ, Reinhart TA, Bartlett D, Kalinski P. Ability of mature dendritic cells to interact with regulatory T cells is imprinted during maturation. Cancer Res. 2008; 68:5972–8. [PubMed: 18632653]
17. Townsend A, Ohlen C, Bastin J, Ljunggren HG, Foster L, Karre K. Association of class I major histocompatibility heavy and light chains induced by viral peptides. Nature. 1989; 340:443–8. [PubMed: 2666863]
18. Prins RM, Odesa SK, Liau LM. Immunotherapeutic targeting of shared melanoma-associated antigens in a murine glioma model. Cancer Res. 2003; 63:8487–91. [PubMed: 14679014]
19. Hatano M, Kuwashima N, Tatsumi T, et al. Vaccination with EphA2-derived T cell-epitopes promotes immunity against both EphA2-expressing and EphA2-negative tumors. J Transl Med. 2004; 2:40. [PubMed: 15563374]
20. Iizuka Y, Kojima H, Kobata T, Kawase T, Kawakami Y, Toda M. Identification of a glioma antigen, GARC-1, using cytotoxic T lymphocytes induced by HSV cancer vaccine. Int J Cancer. 2006; 118:942–9. [PubMed: 16152596]
21. Overwijk WW, Tsung A, Irvine KR, et al. gp100/pmel 17 is a murine tumor rejection antigen: induction of “self ”-reactive, tumoricidal T cells using high-affinity, altered peptide ligand. J Exp Med. 1998; 188:277–86. [PubMed: 9670040]
22. Okada H, Tahara H, Shurin MR, et al. Bone marrow-derived dendritic cells pulsed with a tumor-specific peptide elicit effective anti-tumor immunity against intracranial neoplasms. Int J Cancer. 1998; 78:196–201. [PubMed: 9754652]
23. Sasaki K, Zhu X, Vasquez C, et al. Preferential expression of very late antigen-4 on type 1 CTL cells plays a critical role in trafficking into central nervous system tumors. Cancer Res. 2007; 67:6451–8. [PubMed: 17616706]
24. Zhu X, Nishimura F, Sasaki K, et al. Toll like receptor-3 ligand poly-ICLC promotes the efficacy of peripheral vaccinations with tumor antigen-derived peptide epitopes in murine CNS tumor models. J Transl Med. 2007; 5:10. [PubMed: 17295916]

Author Manuscript Author Manuscript Author Manuscript Author Manuscript

25. Walker PR, Calzascia T, Schnuriger V, et al. The brain parenchyma is permissive for full antitumor CTL effector function, even in the absence of CD4 T cells. J Immunol. 2000; 165:3128–35. [PubMed: 10975826]
26. Banchereau J, Briere F, Caux C, et al. Immunobiology of dendritic cells. Annu Rev Immunol. 2000; 18:767–811. [PubMed: 10837075]
27. Curiel TJ, Coukos G, Zou L, et al. Specific recruitment of regulatory T cells in ovarian carcinoma fosters immune privilege and predicts reduced survival. Nat Med. 2004; 10:942–9. [PubMed: 15322536]
28. Hokey DA, Larregina AT, Erdos G, Watkins SC, Falo LD Jr. Tumor cell loaded type-1 polarized dendritic cells induce Th1-mediated tumor immunity. Cancer Res. 2005; 65:10059–67. [PubMed: 16267032]
29. Feili-Hariri M, Falkner DH, Morel PA. Polarization of naive T cells into Th1 or Th2 by distinct cytokine-driven murine dendritic cell populations: implications for immunotherapy. J Leukoc Biol. 2005; 78:656–64. [PubMed: 15961574]
30. Loetscher M, Gerber B, Loetscher P, et al. Chemokine receptor specific for IP10 and mig: structure, function, and expression in activated T-lymphocytes. J Exp Med. 1996; 184:963–9. [PubMed: 9064356]
31. Dufour JH, Dziejman M, Liu MT, Leung JH, Lane TE, Luster AD. IFN-γ-inducible protein 10 (IP-10; CXCL10)-deficient mice reveal a role for IP-10 in effector T cell generation and trafficking. J Immunol. 2002; 168:3195–204. [PubMed: 11907072]
32. Gattass CR, King LB, Luster AD, Ashwell JD. Constitutive expression of interferon γ-inducible protein 10 in lymphoid organs and inducible expression in T cells and thymocytes. J Exp Med. 1994; 179:1373–8. [PubMed: 8145049]
33. Nakamura Y, Watchmaker P, Urban J, et al. Helper function of memory $CD8^+$ T cells: heterologous $CD8^+$ T cells support the induction of therapeutic cancer immunity. Cancer Res. 2007; 67:10012–8. [PubMed: 17942935]
34. Eguchi J, Kuwashima N, Hatano M, et al. IL-4-transfected tumor cell vaccines activate tumor-infiltrating dendritic cells and promote type-1 immunity. J Immunol. 2005; 174:7194–201. [PubMed: 15905564]
35. Yang T, Witham TF, Villa L, et al. Glioma-associated hyaluronan induces apoptosis in dendritic cells via inducible nitric oxide synthase: implications for the use of dendritic cells for therapy of gliomas. Cancer Res. 2002; 62:2583–91. [PubMed: 11980653]
36. Nishioka Y, Wen H, Mitani K, et al. Differential effects of IL-12 on the generation of alloreactive CTL mediated by murine and human dendritic cells: a critical role for nitric oxide. J Leukoc Biol. 2003; 73:621–9. [PubMed: 12714577]
37. Bronte V, Zanovello P. Regulation of immune responses by L-arginine metabolism. Nat Rev Immunol. 2005; 5:641–54. [PubMed: 16056256]

Author Manuscript Author Manuscript Author Manuscript Author Manuscript

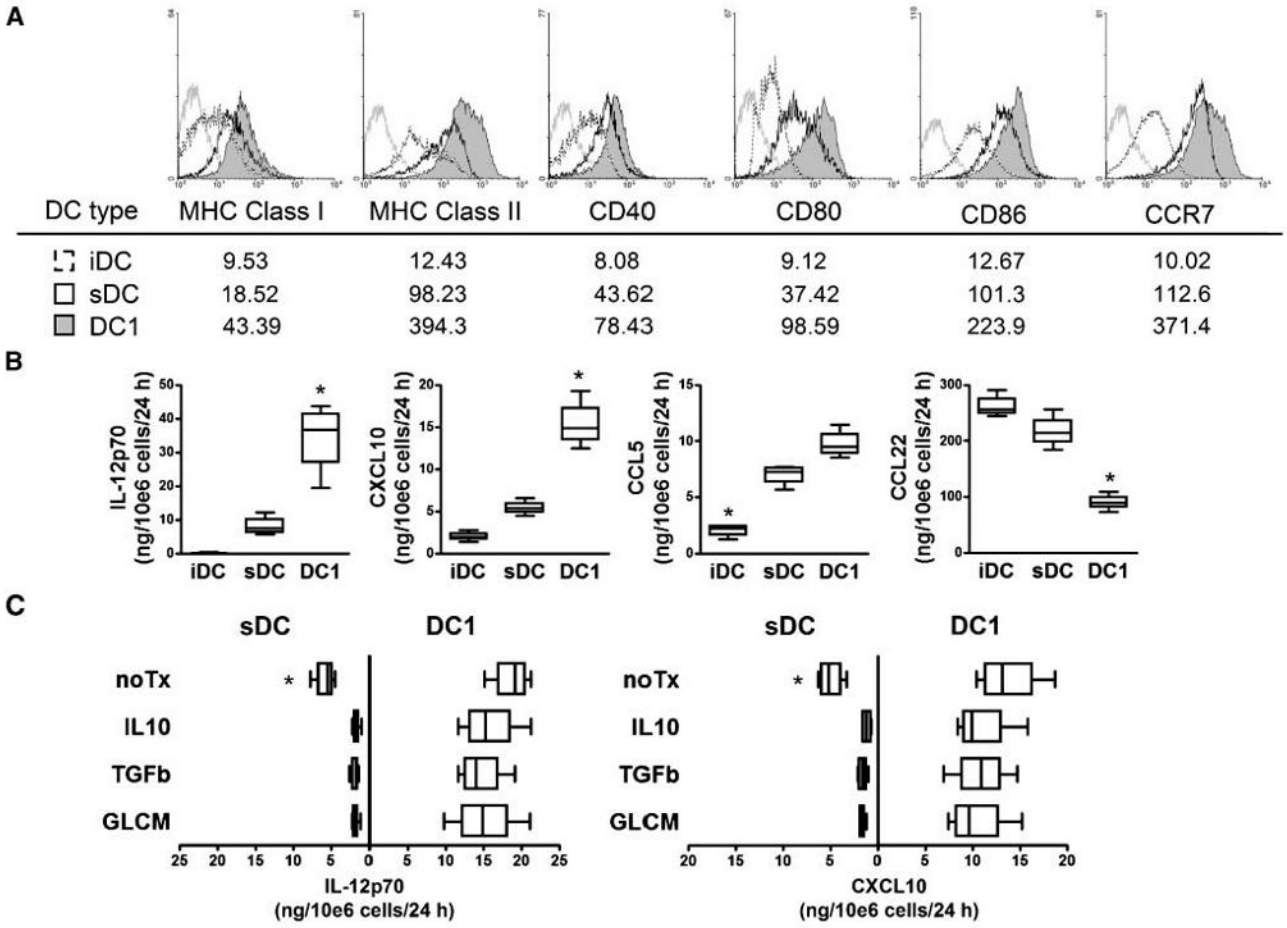

Figure 1.

Mouse DC1s stably retain their type 1 polarizing phenotype when exposed to type 2–promoting or Treg-promoting environments. On day 0, C57BL/6 mouse–derived BMCs were cultured with 10 ng/mL rmGM-CSF. On day 6, iDCs were obtained by positive selection with CD11c magnetic beads; sDCs were then generated by further 24-h cultivation of $CD11c^+$ DCs with 250 ng/mL LPS and 10 ng/mL rmGM-CSF. $CD11c^+$ DC1s were generated from iDC by further 24-h cultivation with 5 μg/mL poly-ICLC and 10 ng/mL each of rmIFN-γ, rmIFN-α, and rmIL-4. *A*, on day 7, $CD11c^+$ cells were evaluated by flow cytometry for DC maturation markers. Histograms represent the following DC types: DC1s (*shaded*), sDCs (*open*), iDCs (*dashed line*), and DCs stained with isotype control IgG (*gray line*). Numbers under each histogram represent mean fluorescent intensity (MFI) for each DC type. *B*, the amount of IL-12p70, CXCL10, CCL5, and CCL22 produced for the last 24 h was evaluated after stimulation of DCs by CD40L-transduced J558 cells. *, $P < 0.05$, compared with other groups with the same DC type. *C*, DC1s and sDCs were subsequently cultured in the presence of either 10 ng/mL rmIL-10, 10 ng/mL rmTGF-β1, or GL261-conditioned medium (*GLCM*) for another 24 h, followed by CD40L stimulation for another 24 h. The amount of IL-12p70 and CXCL10 produced for the last 24 h was evaluated. *, $P < 0.05$ compared with other groups in the same DC type.

Author Manuscript Author Manuscript Author Manuscript Author Manuscript

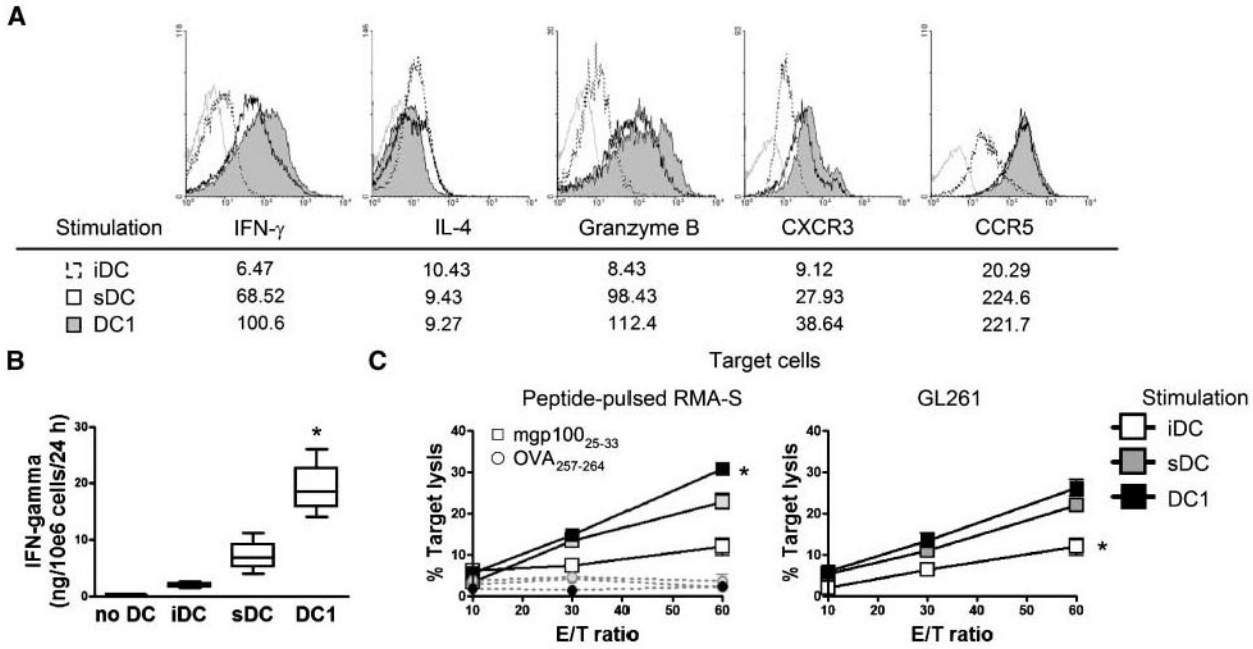

Figure 2.

Mouse DC1s efficiently induce antigen-specific type 1 CTLs *in vitro*. Naive Pmel-I $CD8^+$ T cells were stimulated with DC1s, sDCs, or iDCs loaded with 5 μg/mL $hgp100_{25\text{-}33}$ peptide in the presence of 50 units/mL rhIL-2 for 6 d. *A*, $CD8^+$ T cells were evaluated by flow cytometry for the intracellular expression of IFN-γ, IL-4, granzyme B, CXCR3, and CCR5. Histograms represent T cells stimulated with the following DC types: DC1s (*shaded*), sDCs (*open*), and iDCs (*dashed line*). *Gray lines*, T cells stained with isotype control IgG. Numbers indicated under histograms represent MFI for T cells stimulated with each DC type. *B*, IFN-γ secretion of T cells into the culture medium was evaluated by ELISA. *, $P < 0.05$ compared with other groups. *C*, cytolytic ability of effector T cells against target cells was evaluated by ^{51}Cr releasing assay. *Left*, target RMA-S cells were pulsed with 5 μg/mL of either $mgp100_{25\text{-}33}$ (*square*) or $OVA_{257\text{-}264}$ (*circle*) peptide. *Right*, GL261 cells were used as target cells. *, $P < 0.05$ compared with other groups at the same E/T ratio.

Author Manuscript Author Manuscript Author Manuscript Author Manuscript

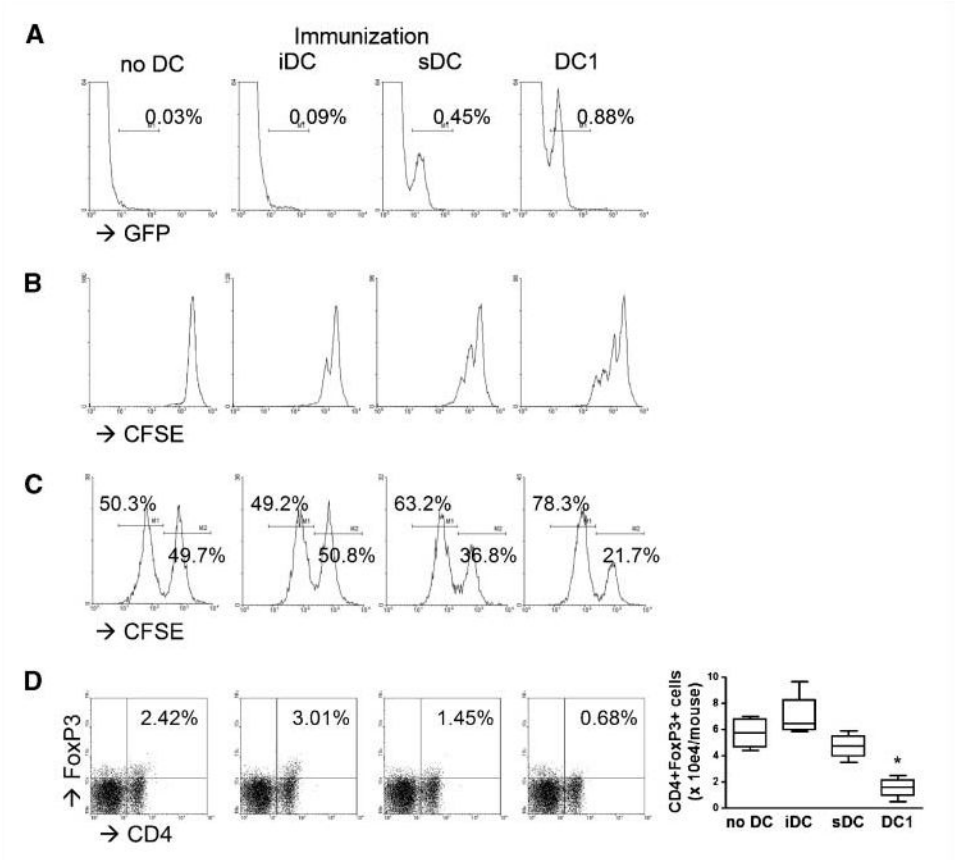

Figure 3.

Mouse DC1s efficiently migrate into DLNs, induce antigen-specific CTLs, and suppress Treg accumulation *in vivo*. On day 0, wild-type mice received s.c. immunization with either DC1s, sDCs, or iDCs. *A*, mice received 3×10^6 GFP^+ DCs. GFP^+ cells in DLNs were evaluated by flow cytometry at 48 h. Numbers in each histogram represent the percentage of GFP^+ cells in monocyte-gated populations. *B*, DCs were loaded with 5 μg/mL $hgp100_{25\text{-}33}$ peptide. On day – 1, mice received i.v. injection of 5×10^6 naive Pmel-I $CD8^+$ T cells labeled with CFSE. On day 6, proliferation of CFSE-positive subpopulations in iDLNs was analyzed. *C*, DCs were loaded with 1×10^6 $Garc1_{77\text{-}85}$ peptide. On day 6, cytolytic ability of effector T cells against target cells was evaluated by *in vivo* cytolytic assay, as described in Materials and Methods. *D*, on day 6, DLNs were evaluated by flow cytometry for $FoxP3^+CD4^+$ cells. Numbers in each dot plot represent the percentage of double-positive cells in lymphocyte-gated subpopulations in DLNs. Absolute numbers of double-positive cells are enumerated in the right box plots. *, $P < 0.05$ compared with other groups.

Author Manuscript Author Manuscript Author Manuscript Author Manuscript

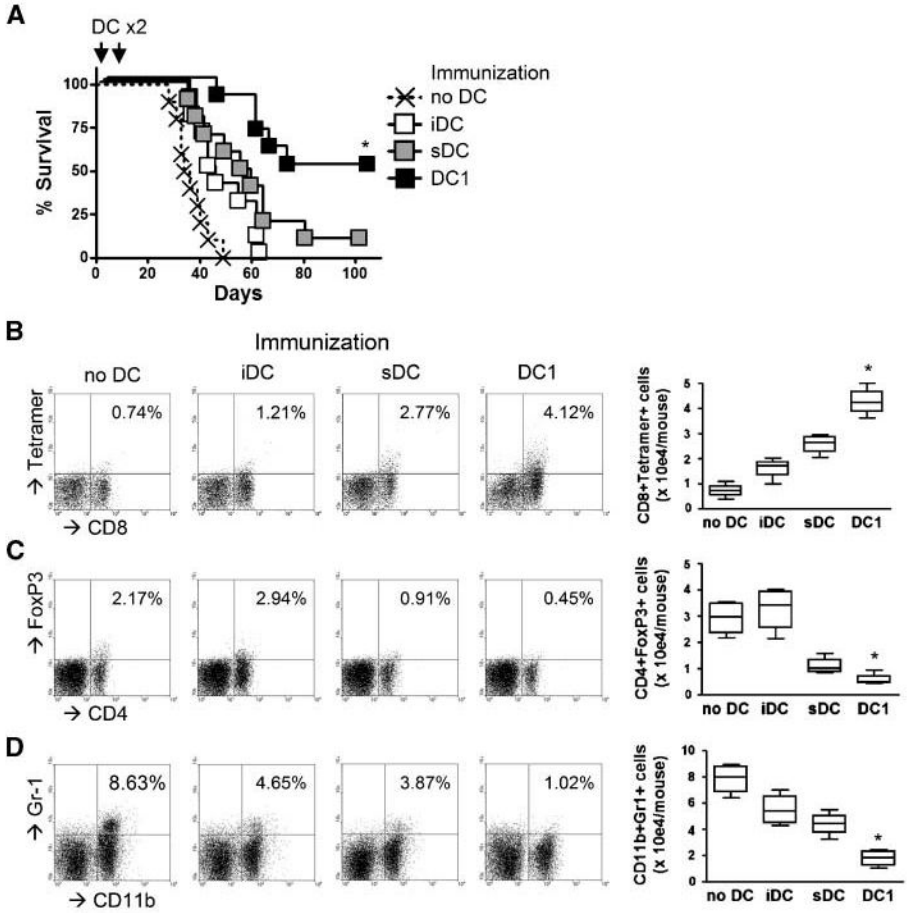

Figure 4.

Peripheral immunization with DC1s prolongs survival of CNS glioma-bearing mice, associated with the efficient CNS glioma homing of antigen-specific CTLs. On day 0, each syngeneic mouse received a stereotactic injection with 1×10^5 GL261 glioma cells into the right basal ganglia. On days 0 and 10, mice received s.c. immunization with 1×10^6 GAA-loaded DC1s, sDCs, or iDCs. *A*, DCs were loaded with a combination of $Garc1_{77\text{-}85}$ and $EphA2_{682\text{-}689}$ peptides. Symptom-free survival was monitored. *, $P < 0.05$ compared with other groups. *B-D*, DCs were loaded with $hgp100_{25\text{-}33}$ peptide. On day –1, mice received i.v. infusion of 5×10^6 naive Pmel-I $CD8^+$ T cells. On day 16, BILs were evaluated by flow cytometry for the following subpopulations: gp100-reactive $CD8^+$ cells (*B*), $FoxP3^+CD4^+$ Tregs (*C*), and Gr-1^+CD11b^+ myeloid suppressor cells (*D*). Numbers in each dot plot represent the percentage of double-positive cells in lymphocyte-gated subpopulations in BILs. Absolute numbers of double-positive cells are enumerated in the right box plots. *, $P < 0.05$ compared with other groups.

Author Manuscript Author Manuscript Author Manuscript Author Manuscript

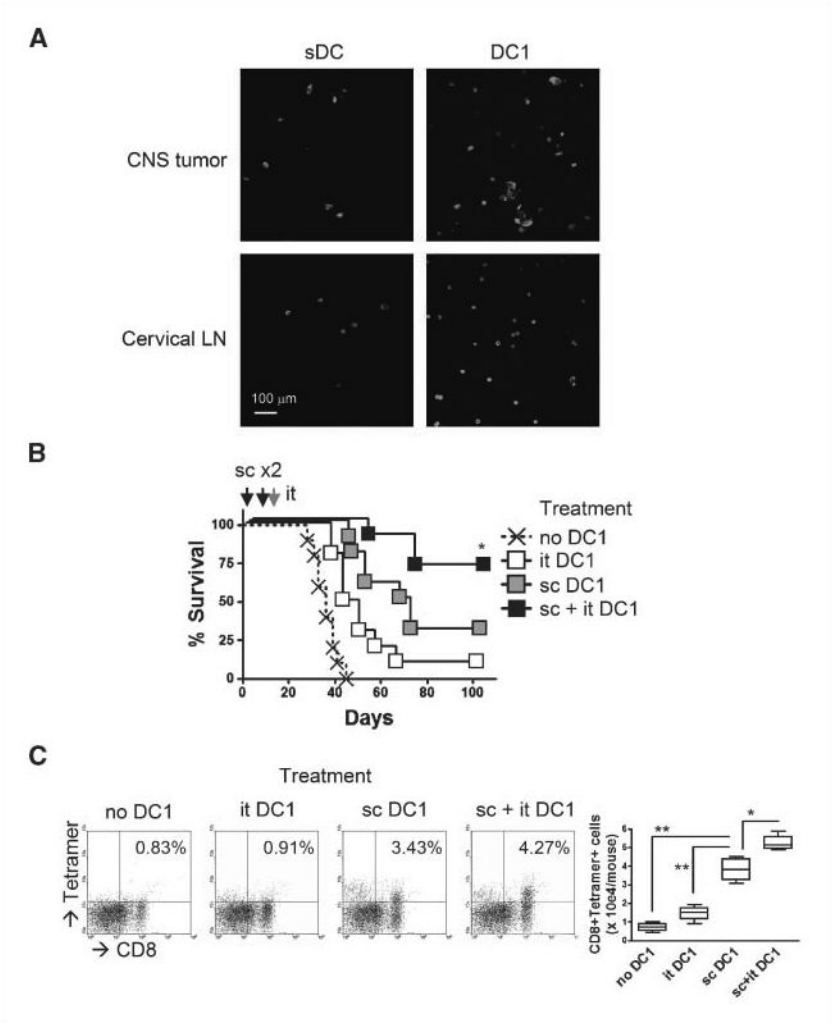

Figure 5.

Intratumoral injection of DC1s enhances anti-CNS glioma effects of s.c. immunization with DC1s. *A* mice bearing day 21 CNS GL261 glioma received i.t. injection of 3×10^6 GFP^+ DC1s or GFP^+ sDCs. On day 27, brain sections and ipsilateral CLNs were evaluated by two-photon microscopy for GFP^+ cells. Original magnification, 60×. *B* and *C*, mice received either one of the following combinations: (*a*) s.c. PBS and i.t. PBS, (*b*) s.c. PBS and i.t. GAA-loaded DCs, (*c*) s.c. GAA-loaded DCs and i.t. PBS, or (*d*) s.c. GAA-loaded DCs and i.t. GAA-loaded DCs. For s.c. immunization on days 0 and 10, 1×10^6 GAA-loaded DC1s were injected with 100 μL PBS; for i.t. injections on day 16, 1×10^6 GAA-loaded DC1s were injected with 2 μL PBS. *B*, DCs were loaded with a combination of $Garc1_{77\text{-}85}$ and $EphA2_{682\text{-}689}$ peptides. Symptom-free survival was monitored. *, $P < 0.05$ compared with other groups. *C*, DCs were loaded with $hgp100_{25\text{-}33}$ peptide. On day –1, mice received i.v. injection of 5×10^6 naive Pmel-I $CD8^+$ T cells. BILs were evaluated by flow cytometry on day 21 for gp100-reactive $CD8^+$ cells. Numbers in each dot plot represent the percentage of double-positive cells in lymphocyte-gated subpopulations in BILs. Absolute numbers of double-positive cells are enumerated in the right box plots. *, $P < 0.05$ compared with sDC group; **, $P < 0.01$ compared with no DC1 and i.t. DC1 groups.

Author Manuscript Author Manuscript Author Manuscript Author Manuscript

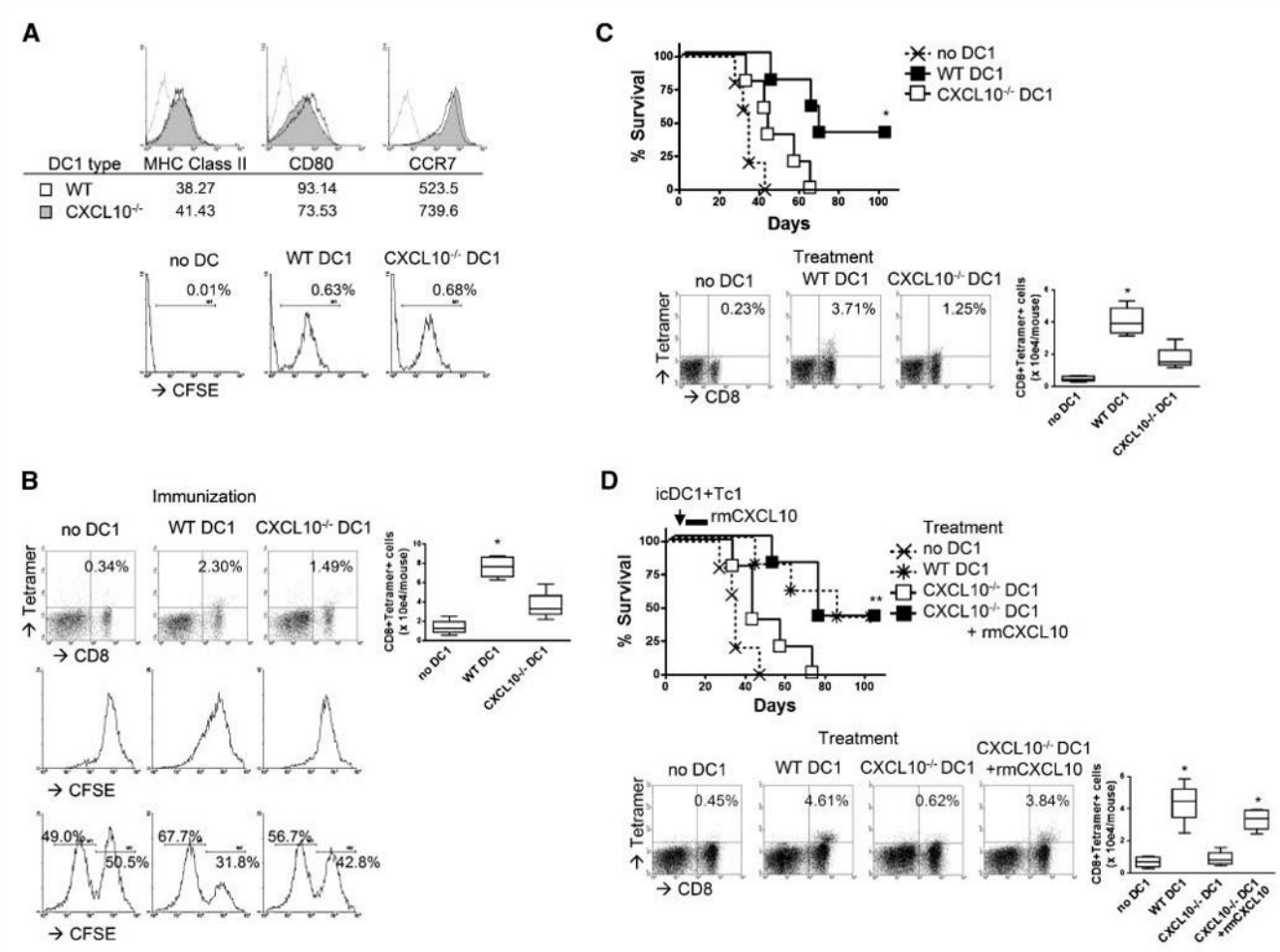

Figure 6.

DC1-derived CXCL10 plays a significant role in both induction of antigen-specific CTLs and their CNS glioma homing. DC1s were generated from either wild-type or *CXCL10*$^{-/-}$ mice. *A, top*, CD11c^{+} cells were evaluated by flow cytometry for DC maturation markers. Histograms represent the following DC types: *CXCL10*$^{-/-}$ DC1s (*shaded*), wild-type DC1s (*open*), and DCs stained with isotype control IgG (*gray line*). Numbers indicated under each histogram represent MFI for each DC type. *Bottom*, on day 0, wild-type mice received s.c. immunization with 3×10^{6} CFSE-labeled DC1s. CFSE^{+} cells in DLNs were evaluated by flow cytometry at 48 h. Numbers in each dot plot represent the percentage of double-positive cells in monocyte-gated subpopulations in DLNs. *B*, on day 0, wild-type mice received s.c. immunization with GAA-loaded DC1s. *Top and center*, DCs were loaded with 5 μg/mL hgp100$_{25\text{-}33}$ peptide. On day –1, mice received i.v. injection of naive Pmel-I CD8^{+} T cells. *Top*, on day 6, DLNs were evaluated by flow cytometry for gp100-reactive CD8^{+} cells. Numbers in each dot plot represent the percentage of double-positive cells in lymphocyte-gated subpopulations. *Center*, T cells injected were labeled with CFSE. On day 6, proliferation of CFSE^{+} cells were evaluated by flow cytometry. *Bottom*, DCs were loaded with 1×10^{6} Garc1$_{77\text{-}85}$ peptide. On day 6, cytolytic ability of effector T cells against target cells was evaluated by *in vivo* cytolytic assay, as described in Materials and Methods. *C*, on

Author Manuscript Author Manuscript Author Manuscript Author Manuscript

days 0 and 10, CNS glioma-bearing mice received s.c. immunization with GAA-loaded DC1s. *Top*, DCs were loaded with a combination of $Garc1_{77-85}$ and $EphA2_{682-689}$ peptides. Symptom-free survival was monitored. *, $P < 0.05$ compared with other groups. *Bottom*, DCs were loaded with $hgp100_{25-33}$ peptide. On day –1, mice received i.v. injection of naive Pmel-I $CD8^+$ T cells. On day 16, BILs were evaluated by flow cytometry for gp100-reactive $CD8^+$ cells. *D*, on day 12, CNS glioma-bearing mice received i.t. injection of $hgp100_{25-33}$-loaded DC1s and i.v. injection of Pmel-I–derived, *ex vivo*–expanded type 1 CTLs. For a group of *CXCL10*$^{-/-}$ DC1s, 1 μg rmCXCL10 in 1 μL PBS was i.t. injected on days 12, 15, and 18. *Top*, symptom-free survival was monitored. **, $P < 0.05$ both wild-type (*WT*) DC1 and *CXCL10*$^{-/-}$ DC1 with rmCXCL10groups compared with either no DC control or *CXCL10*$^{-/-}$ DC1 groups. *Bottom*, BILs were evaluated by flow cytometry on day 21 for gp100-reactive $CD8^+$ cells. *B–D*, numbers in each dot plot represent the percentage of double-positive cells in lymphocyte-gated subpopulations in BILs. Absolute numbers of double-positive cells are enumerated in the right box plots. *, $P < 0.05$ compared with other groups (*B* and *C*) and compared with no DC1 and *CXCL10*$^{-/-}$ DC1 groups (*D*).